River Flow 2010 - Dittrich, Koll, Aberle & Geisenhainer (eds) - © 2010 Bundesanstalt für Wasserbau ISBN 978-3-939230-00-7

Experimental investigation on the sediment movement in the vicinity of a cylindrical bridge pier

F. Pfleger & Ch. Rapp & M. Manhart
Fachgebiet Hydromechanik, Technische Universität München, Germany

ABSTRACT: An experimental investigation on sediment movement pattern in a developing scour hole in the vicinity of a cylindrical pier by image processing techniques is presented. A new algorithm based on investigations by Papanicolaou et al. (1999) and Radice et al. (2006b) has been implemented. A sediment-embedded cylindrical pier (D=0.10 m) was placed 16 m downstream from the inlet of a 1.2 m wide laboratory flume. The sediment is considered to be uniform (σ_g=1.14) and its mean diameter is d_{50}=1.9 mm. 20% of the sediment grains were coloured black to assure a significant contrast. The pictures of the sediment surface were captured by a CMOS-camera at $1.3x10^6$ pixels from above through a plexiglass plate which was slightly submerged onto the water surface. The scour hole was therefor lighted continuously. For the evaluation of the image sequences a combination of difference images and a particle identification algorithm is used to find moving black grains. The corresponding particle in the consecutive frame is found via a correlation coefficient containing grayscale similarity, deviation from the most probable moving direction and exclusion of white grains moving on black background. The presented experiment was conducted for 20 hours at 80% of the critical section averaged velocity at 0.15 m flowdepth. For several times during the experiment a sequence of 10,000 frames was captured. Time-averaged moving directions and histograms of the moving directions in the pier vicinity and their evolution in time at a high spatial resolution will be provided and discussed.

Keywords: pier scour, sediment movement, particle tracking

1 INTRODUCTION

The scouring process in the vicinity of a cylindrical pier has been intensively studied during the last decades. The main goal of the research in this field is to provide tools to predict the maximum scour depth and its evolution in time for certain flow and sediment conditions. Many, mainly experimental, investigations on the flow field and the influence of different parameters on the scouring process have been conducted. However, the formulas for the assessment of the scour depth yielding from these different works still differ considerably in certain applications (Link (2006)). Further investigations leading to a deeper understanding of the scouring process are therefore essential.

For the description of the temporal evolution of the scour depth it is important to know the main scouring agents, their impact on the erosion process and their evolution in time. The erosion process has been described qualitatively in several works (e.g. Melville (1975), Zanke (1982)). For a more detailed analysis of the sediment transport measurements of the particle movement providing a high spatial resolution are necessary. The application of image processing techniques is a suitable way to gain these data.

During the last years measurement systems using image processing techniques had a growing impact on experimental investigations in fluid mechanics. The most mature ones are Particle Image Velocimetry (PIV) and Particle Tracking Velocimetry (PTV) which allow the measurement of particle movements representing fluid velocities. Furthermore in some works these principles were used to measure the sediment movement.

These works can be split up in two groups: one recording the sediment surface from above and one capturing the sediment bed from besides. For the analysis of the pier scour process a method belonging to the first group has to be used. Several

researchers developed measurement systems for this method. Pilotti et al. (1997) tracked sediment grains on the flume bottom using a software algorithm for the analysis. Sechet and Le Guennec (1999) developed a system to detect grain movements on transparent flume bottoms. Keshavarzy and Ball (1999) located particle movements on a natural sediment bed counting the moving grains manually and Papanicolaou et al. (1999) conducted a software based analysis of the movement of coloured glass spheres on transparent ones. Radice et al. (2006a), (2006b) and (2008) developed a system for a software based analysis of the sediment kinematics in the vicinity of an abutment using PIV methods.

In this paper a new measurement system for the detection of grain movements on natural sediment surfaces is presented. It has been utilised to map the movement pattern in the vicinity of a cylindrical pier at different stages of the scouring process.

2 EXPERIMENTAL SETUP

2.1 *Flume*

The experiments were conducted in the Hydromechanics Laboratory of Technische Universität München. The flume was 1.20 m wide and 1 m deep. In the downstream part of the flume an elevated bottom is mounted and a working section is placed 16 m downstream from the inlet. In the center of this section a cylindrical pier (diameter D = 0.10 m) is embedded in a 0.3 m deep sand bed. 6.5 m upstream of the pier the elevated bottom is covered by a sediment layer to ensure the development of an adequate boundary layer. The discharge was adjusted by a gate in the inflow pipe and the flow depth by a sluice at the end of the flume. Close to the inlet and at the beginning of the elevated bottom two flow straighteners of different mesh size were mounted. A sketch of the flume is shown in Figure 1. A detailed description of the measurement section is given in chapter 2.4.

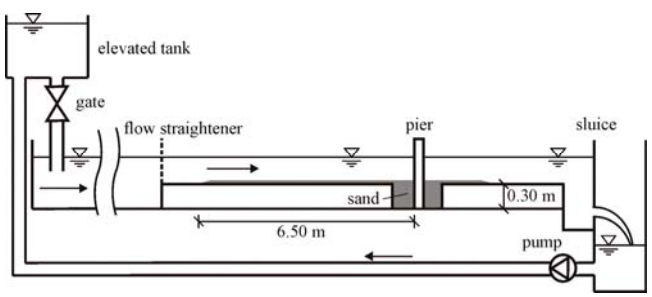

Figure 1. Sketch of the flume setup.

2.2 *Sediment*

Natural coarse sand is used as sediment. The representative diameter is $d_{50} = 1.9$ mm. Since $\sigma_g = \sqrt{d_{84.1}/d_{15.9}} = 1.14$ the sediment can be considered to be uniform. The angle of repose is approximately 30°. To provide a significant contrast 20% of the sediment grains were coloured black (see Chapter 3.1).

2.3 *Flow conditions*

All experiments in this study were conducted at a flow depth of 0.15 m. Preliminary experiments were conducted in the flume to assess the critical conditions for the sediment movement in an undisturbed channel flow. Thereby the critical bed shear stress was found to be $\tau_{cr} = 0.59$ N/m² corresponding to a section averaged velocity of 0.42 m/s under the assumption of a fully developed logarithmic velocity profile. The final investigations were made at 80% of the critical velocity.

2.4 *Camera and lightening*

The images of the sediment surface were captured by a monochrome CMOS-camera with maximum $1.3 \cdot 10^6$ pixel at a variable frame rate. Due to the limited data transfer rate the maximum frame rate depends on the image size. In the actual study the frame rate was 27 fps. The pixel values were saved at 8-bit precision (ranging from 0 to 255).

To ensure a defined optical access to the sediment surface a plexiglass plate was slightly submerged onto the water surface. Accoring to Radice et al. (2008) the effect of the pressurized flow introduced by the plate on the characteristics of the scouring process is negligible.

The mapped sediment area was lighted continuously with two spotlights from above and an additional light source inside the transparent pier. This arrangement ensured an equal distribution of the light intensity in the whole frame also for a developing scour hole. The measurement section was shaded to avoid influences from the lightening in the proximity on the light intensity at the sediment bed.

The vicinity of the pier was recorded in two frames due to the relation of grain size to pixel size (see Chapter 3.2 for detailed description). These frames covered one side of the axissymmetric scour hole. The borders of the images lay about 0.21 m upstream, 0.14 m downstream and 0.23 m besides the pier axis. These dimensions include the complete scour hole for all scouring stages in the upstream half and the most interesting part in the downstream half.

In Figures 2 and 3 sketches of the measurement section are shown.

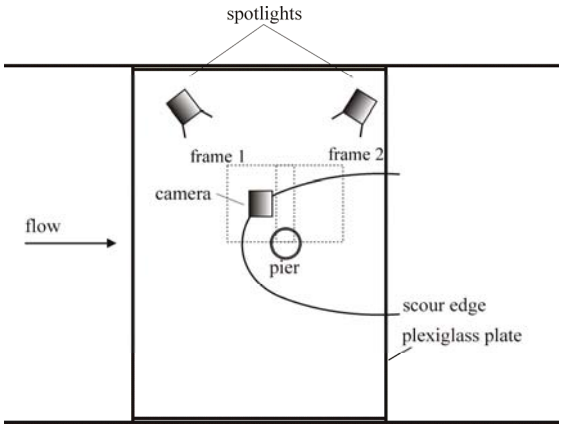

Figure 2. Measuring section, top view.

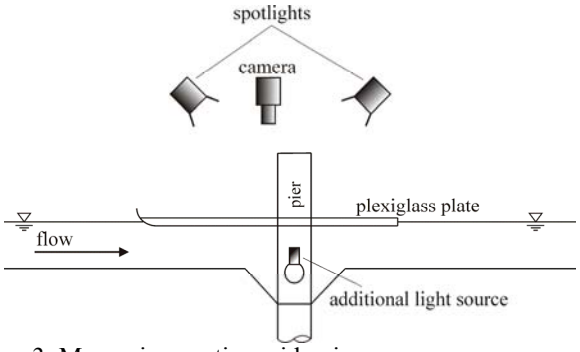

Figure 3. Measuring section, side view.

3 IMAGE PROCESSING

The image sequences captured in this setup are subsequently analysed by digital image processing techniques to detect the movement of sediment grains. In this chapter the algorithm which has been developed for this task and the guidelines for the image recording resulting from this method are explained.

3.1 *Algorithm*

The algorithm is based on the comparison of two consecutive images. Therefore difference images of these frames are calculated by subtraction of the intensity matrices. Assuming that the light intensities in both frames are exactly the same only the regions where grains were displaced are unequal to zero.

For natural sediment problems can appear if a moving grain has only a slight contrast to the background. Additionaly, if it moves from a brighter region (with respect to its color) to a darker region the values in the difference images have the opposite sign. Thus the grain can disappear in the following difference image depending on the subtraction method.

To avoid these problems 20% of the grains used in this experiment were coloured black. The coloured grains were dried carefully to avoid clustering and to assure that the black grains have the same grain size distribution as the original sediment. These black grains move for almost all cases above a brighter background. The algorithm developed for this study is adapted to this fact and detects only the movement of black grains. The fraction of black grains in the sediment is the result of preliminary tests. It is a compromise between the positive effects of a higher fraction of black grains (higher number of moving black grains in the scour and thereby more samples) and its negative impacts (more movement above black background, leads to worse contrasts, less distinct correlation of detected grains in consecutive frames).

In the following the single steps of the image processing are explained. Their results can be seen in Figure 4.

For each time step one pair of consecutive images is analysed. The pixel matrix of image 1 shall be A, the matrix of image 2 B (Figure 4a). First a threshold is substracted from A and B as also proposed in Papanicolaou et al. (1999). This threshold has to be adapted in a way that after the subtraction all black-coloured grains have a negative value. In the resulting matrix all negative values are set to zero, all positive to 255. Thereby Figure 4b is produced, where all black grains appear black and the natural grains white. With these matrices A(b)) and B(b)) two difference images are produced. The first image A(c)) equals A(b)) minus B(b)) and the second image B(c)) equals B(b)) minus A(b)). Both matrices are multiplied by minus one and subsequently negative values are again set to zero. Thereby all moving black grains can be seen in their first position in A(c)) and in their second position in B(c)). All non-moving black grains are zero.

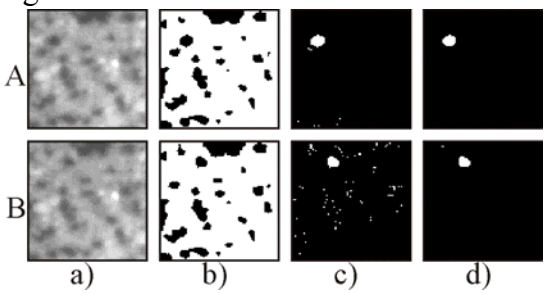

Figure 4. Consecutive steps in image processing

After that a median filter is applied to A(c)) and B(c)) to remove the non-zero values produced by electronical noise as mentioned before (see Papanicolaou et al. (1999)). The result is shown in Figure 4d.

The remaining non-zero spots are analysed. As proposed by Radice et al. (2006b) only clusters of

a certain number of connected non-zero pixels are considered to be grains. The centeroids of these pixel clusters are assumed to be their position.

To find corresponding grains in the two frames first a maximum movement distance is defined. This value has to be adjusted to the maximum sediment velocities, the frame rate and the reproduction scale. Unlike in the experiment of Papanicolaou et al. (1999) the movement direction of the grain can not be predetermined in a scour hole. Hence for all grains in frame B within this distance to one grain in frame A a correlation coefficient is set up to determine the probability that one is the corresponding grain. Three criteria are contributing to this coefficiant. All these criteria are represented by a factor which varies between 0 (no correlation) and 1 (perfect correlation).

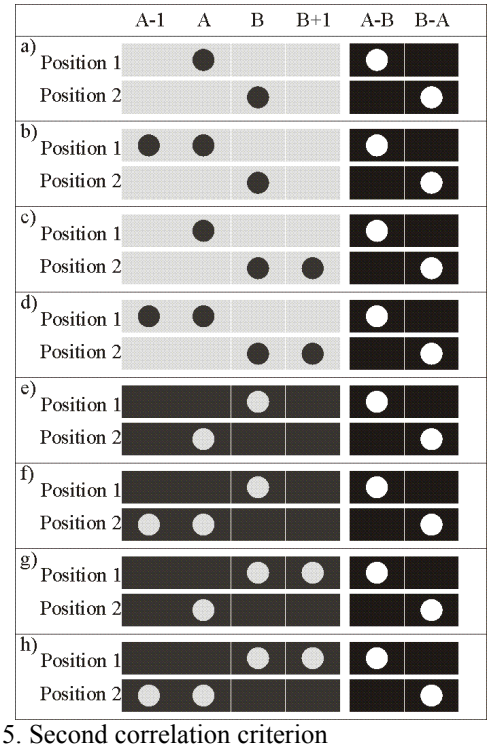

Figure 5. Second correlation criterion

1. The first criterion is the difference of the mean grayscale values of the grains in the original pictures. Its factor FGSV is calculated as

$$FGSV = 1 - \left(\frac{\Delta GSV}{\Delta GSV_{max}} \right) \quad (1)$$

where ΔGSV is the mean grayscale-value difference and ΔGSV_{max} is the user defined maximum difference. If ΔGSV is greater than ΔGSV_{max} FGSV is set to zero.

2. The second criterion is necessary since movements of natural coloured grains on a background of black grains can appear.

If a bright grain moves away from a black background to another position which also has a black background the grayscale value information in the difference images will be the same as if a black grain was moving on the same path just in the opposite direction. To avoid the detection of this virtual movement the image preceeding frame A and the image following frame B are included in the analysis. Figure 5 shows cases of particle movements on brighter or darker background between position 1 and position 2 in a series of four pictures which all result in the same difference images A-B and B-A shown on the right hand side. For all these cases a movement from position 1 to 2 will be detected which is only right for the events a)-d). To exclude e)-h) the mean grayscale values of the pixels where the moving particle is located in A-B and B-A are compared. For a)-d) there is always a difference for these pixels between A and B+1 at position 1 and between A-1 and B at position 2. By contrast, in the cases e)-g) at least one of these two differences becomes zero. Therefore the second factor FWOB is zero if one of the two differences turns to zero and is one if not. Case h) is an exception of this rule. Hence for all movements which pass the first check the difference of A-1 and A at position 1 and of B and B+1 at position 2 are calculated. If both values become zero FWOB is set to zero, if not the factor stays one. Thus also case d) is excluded which can not be avoided by this method.

3. Additionally a statistical criterion is introduced. Therefore a preliminary evaluation of the image sequence is conducted using the correlation criteria one and two. The resulting vector field is separated in interrogation areas and for these areas the mean vectors and the standard deviation are calculated. In a second iteration for all grains within the maximum movement radius the discrepancies of their two displacement components to the most probable displacement (mean vector of first iteration step) are evaluated. These discrepancies are weighted by the standard deviation. Thereby this criterion is weakened in regions where many different movement directions can appear like e.g. in the wake of the cylinder. One factor for each component is calculated by Formula (2)

$$FSTAT(u) = 1 - WSTAT \cdot abs\left(\frac{u_{avg} - u_{grain}}{STD(u)} \right) \quad (2)$$

where WSTAT is a user defined weighting factor, u_{avg} is the mean movement in x-direction, u_{grain} is the movement component in x-direction of the inspected grain and STD(u) is the standard deviation of the u-component in the interrogation area. The factor FSTAT is calculated by averaging FSTAT(u) and FSTAT(v).

The correlation criterion COR is finally calculated by multiplication of the three factors.

$$COR = FGSV \cdot FWOB \cdot FSTAT \quad (3)$$

The highest COR value of all particles in the maximum movement radius is chosen to belong to the corresponding particle in the second difference image if the value is higher than a user defined minimum. Additionally a minimum amplitude ratio of the highest and the second highest COR value can be defined.

Finally the movement distance and thereby a velocity can be calculated with the positions of two corresponding particles.

3.2 *Consequences for image capturing*

The characteristics of this method of image processing defines certain requirements for the image capturing.

The frame rate of the image sequence has to be adjusted to the grain velocities. At a certain velocity a low frame rate leads to large movement distances and thereby to an increasing number of possibly corresponding grains. Increasing the frame rate the displacements can even get smaller than the grain size. The overlapping part of the grains is then not visible in the difference images. That leads to very small pixel clusters which do not fulfill the size criterion of a grain.

The size of the sediment grains in terms of numbers of pixels representing the grain is also very important. Since the black coloured grain must be clearly distinguished from the background their grayscale value must be as low as possible. Pixels lying at the edge of a grain represent partly the grain and partly the brighter background. Thereby they always have a higher value than pixels in the center of a grain. Hence, to ensure a significant contrast, the picture of a grain must be large enough to consist not only of edge pixels.

These two parameters determine the reproduction scale and the frame rate via the camera characteristics.

3.3 *Perspective calibration*

During the scouring process the sediment surface moves away from the camera. Therefore the horizontal coordinate on the sediment surface that is represented by a certain pixel is changing. To find the real position of a grain the geometry of the scour hole has to be mapped for the recorded stage.

For each scouring stage that has been analysed the scouring process has been started from a flat sediment bed and stopped at the relevant time. Afterwards the scour surface has been mapped by a laser distance sensor vertically from above through the plexiglass plate in a 0.005 m cartesian grid. As stated by many researchers (e.g. Dargahi (1987), Dey (1999), Link (2006)) the slopes of the scour hole are stabilised by the horseshoe vortex (HV) and can thus be steeper than the angle of repose. These stabilising forces diminish when the flow is stopped for the geometry measurements. Tests for this scouring configuration showed that the steep slopes at the scour bottom occur only temporarily since the stabilising HV-system seems to be very instable (e.g. Kirkil et al. (2008), Link et al. (2008a)). Therefore the error that is made by stopping the flow is very small compared to the temporarily averaged slope. Geometry measurements of scour slope profiles before and after stopping the process have been made and the results showed only minor differences.

The geomerty data $\Delta z(x,y)$ are used to make a coordinate transformation from the pixel coordinates in the image plane to real horizontal coordinates. As reference point the center of the image plane is chosen (see Figure 6). All heights $\Delta z(x,y)$ are expressed relative to the height z at the reference point. Knowing the height of the lens above the reference point the coordinates of the geometry measurement grid can be transformed to the image plane by intersept theorems. For each moving grain the four closest grid points in the image plane to the grains centeroid are taken to interpolate the height Δz at the grain position. This height is then used to find the real horizontal position of the grain on the sediment surface again via intersept theorems.

One-dimensionally this method is shown in Figure 6, where *dx* is the real position of one grid point, *dpx* its position in the image plane, *dgrain* is the real position of the moving grain and *dpgrain* its position in the image plane.

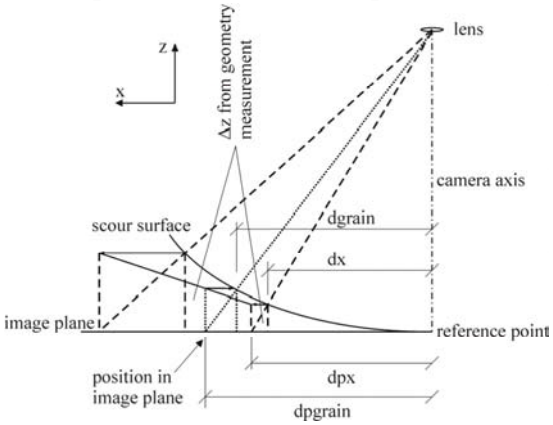

Figure 6. Coordinate transformation in image plane

3.4 *Postprocessing*

As a result of the image analysis the temporarily and spatially averaged movement direction in the interrogation areas are calculated. In Figure 8 the

raw vector field after 0.5 h of scouring is shown exemplarily. Due to low movement intensities in some regions of the scour, the number of samples is not high enough to provide a smooth vector field. Thus a median filter including eight neighbours of one interrogation area is applied to both velocity components. The raw vector field of averaged grain movements is shown in Figure 7 and the result of this operation in Figure 8. It can be seen that the filter is smoothing the field and not changing the tendencies of the raw result.

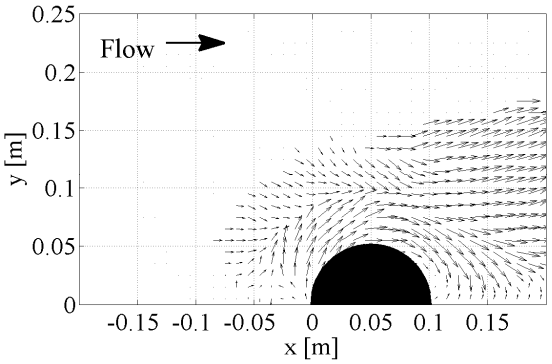

Figure 7. Raw averaged vector field after 0.5 h

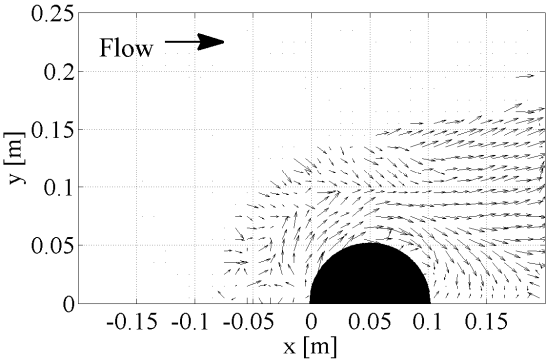

Figure 8. Median filtered averaged vector field after 0.5 h

4 RESULTS

In the following chapter the results of the sediment movement measurements 0.5 h and 12 h after the start of the scouring process are shown. Thereby a comparison between the movements in a rapidly growing and in a developed scour hole is provided. For both stages between 40,000 and 50,000 pictures have been captured at a frame rate of 27 Hz and analysed. According to chapter 3.2 in this setup histograms of the movement velocities show that for high velocities the detection range of the algorithm is wide enough to allow the identification of all movements. For the lower end of the spectrum velocitiy magnitudes below 0.025 m/s are not detected. Assessing equation (13) of van Rijn (1984) for the mean particle velocity this value is exeeded by all transport events where approximately $\tau/\tau_c \geq 1.02$.

The scour experiment has been conducted several times since the recording of 40,000 frames takes approximately 18 minutes. Especially in the initial stage the changes of the scour hole geometry are significant during this time periode. Hence at most 10,000 frames were captured at the early stages in one experiment. This high number of images is necessary since only the movement of 20% of the grains can be detected and some regions in the scour hole have very low movement intensities. Since in a developed scour the intensities decrease even longer image sequences are needed to provide a satisfactory statistic.

The development of the scour hole shows the typical logarithmic shape. The two presented times of the scouring process belong to the initial stage (0.5 h) and the final stage (12 h) (Link (2006)). The differences of the sediment movement will be discussed in the following chapter.

4.1 *Averaged movement directions and sediment velocities*

Figure 9 and Figure 10 show the averaged sediment movement directions and velocities in the scour hole after 0.5 h and 12 h respectively.

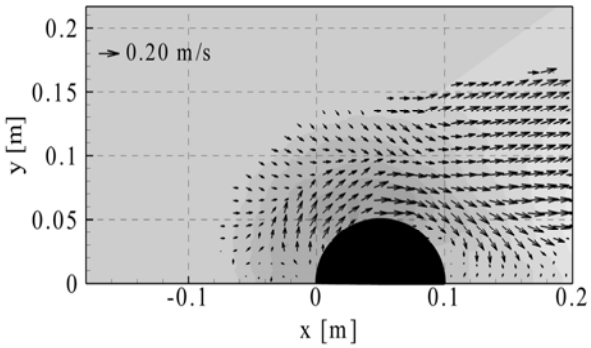

Figure 9. Averaged vector field after 0.5 h

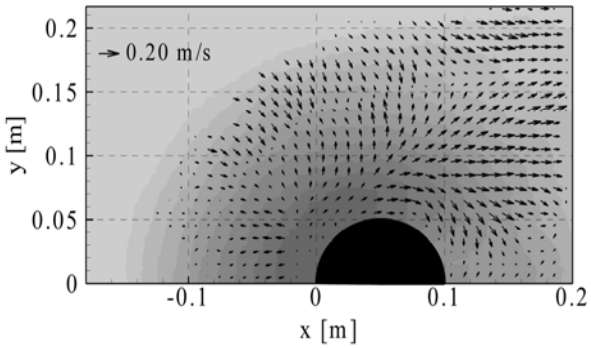

Figure 10. Averaged vector field after 12 h

Only one half of the symmetric scour hole is represented. The axis of symmetry of the scour and the channel is at y = 0. The water flows from the left to the right. A reference for the vector

scale is shown in the upper left corner. The scour hole contour is shown in the background.

The topography of the scour hole in the initial stage shows the deepest point at the pier side as stated by many researcher (e.g. Link et al. (2008b)). In the downstream part the displaced grains are deposited and form a small hill above the original level of the sediment bed. In the developed scour hole the deepest point is located at the pier front and the deposition hill has been transported downstream. Therefore the scour hole is streched to the end of the captured area.

At the early stage with a high deepening rate of the scour high grain velocities appear close to the pier at about 45° to 80° from the plane of symmetry on the upstream side of the pier. This is the area where the scouring process starts and where the highest shear stresses occur during the initial stage (Hjorth (1975)). The tangential component of these vectors is dominant in the initial stage. The HV-system is not completely developed. Outside this region in the upstream part radial movement caused by grains sliding down the scour slope occurs. Downstream the pier the streamwise flow component controls the transport. The slope of the deposition hill behind the pier leads to a sightly diverging vector field. The grains are transported downstream and due to the spanwise inclined surface they are at the same time sliding down the slope. In the detachement zone in the wake of the cylinder the mean velocities are very small since the movements in this area do not have a main direction. The instantaneous velocities are significantly higher.

In the developed scour hole the grain velocities in general are lower than in the inital stage. Between 0° and 90° from the plane of symmetry only the vectors close to the pier have a dominant tangential component. Further away from the pier the HV-system mainly controls the transport. In this area the mean directions point radially away from the cylinder axis. The grains are transported uphill to a certain height. Above this level the movement is dominated by grains sliding down the slope which is represented by radial vectors towards the pier. Following this area around the pier the vectors contain more and more streamwise components. In this region the velocity field of the HV-system and the avalanches in the upper part of the slope are superposed by the main flow. The grains transported out of the scour in the downstream part move almost directly in the streamwise direction.

4.2 *Angle histograms of movement directions*

In some areas of the scour hole the averaged movement components are very small. Despite the region where grain velocities are low this also appears in regions were the grains are moving in many different directions. Therefore Figure 11 and Figure 12 show the histograms of the movement direction in the interrogation areas after 0.5 h and 12 h respectively. The angle histograms are conventional histograms of all occuring movement directions of all grains moving in the corresponding interrogation area. They are plotted in polar coordinates to clarify the kinematics. The width of the histogram classes is 20°. The length of the bars corresponds to the number of grains transported in the according direction weighted by their velocity. Thereby besides the kinematics also information about the transport rate is provided. Figure 11 and Figure 12 show an overview of the complete scour hole.

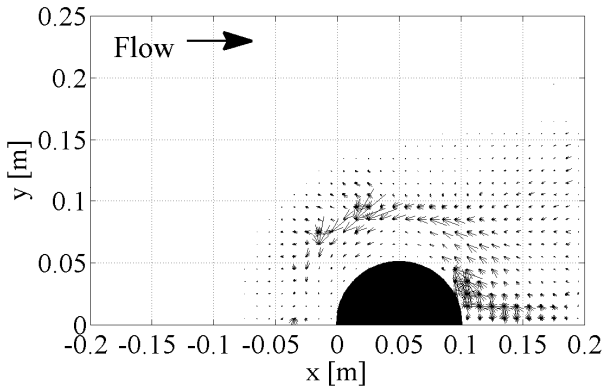

Figure 11. Weighted angle histograms after 0.5 h

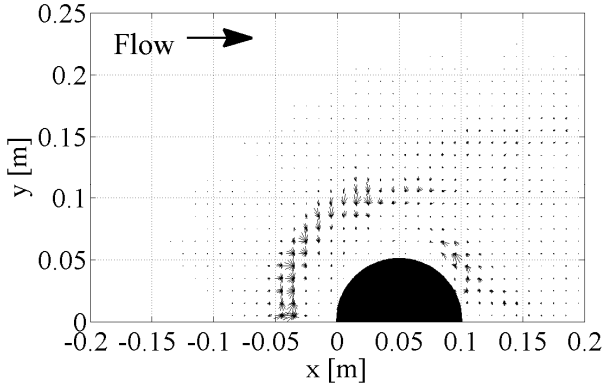

Figure 12. Weighted angle histograms after 12 h

Both scouring stages show a circular region in a radial distance of approximately 0.09 m from the cylinder axis where the main transport is taking place. After 0.5 h this transport is mainly directed tangentially. The main flow dominates the grain movement but its erosive capacity is acting a few centimeters away from the pier. This fact points to a flow situation with a weak HV-system already established and stretched around the pier foot. This vortex covers the sediment surface close to

the pier and keeps the main flow away from this area.

In the developed scour hole most of the grains in the high transport region move in radial direction uphill driven by the now fully established HV-system. There are also movements in tangential direction but especially between 0° and 30° from the plane of symmetry these point into both azimuthal directions. Following this

region around the pier the tangential component is more and more directed downstream. In this sector high turbulent shear stresses produced by the HV-system are acting. Above this ring the movement is dominated by sliding grains and below the absolute number of transported grains is very low and their direction mainly tangential.

Especially after 0.5 h in the wake of the pier the detachement zone can be localised where the grains move in almost all directions at a high movement intensity. As noted in Chapter 4.1 the resulting mean value is very small in this area and therefore the effective transport is very low. The movement intensities in the wake of the pier are also decreasing during the scouring process.

The total transport intensities represented by the histograms are significantly smaller in a developed scour hole.

5 CONCLUSION

In this work a new algorithm for the image processing based measurement of sediment movement is presented. The method uses difference images to detect grain movements and a correlation factor to find the corresponding grains in successive frames. The algorithm identifies the movement of dark grains which were coloured black and mixed with the natural sediment. This ensures a significant contrast and explicit correlations between grains in different images.

A pier scour experiment with a cylindrical pier was conducted in a laboratory flume with a uniform sediment (coarse sand) at 80% of the section averaged critical flow velocity.

The image sequences were captured from vertically above through a plexiglass plate which was slightly submerged onto the water surface. The sediment surface was lightened continuously.

The distortions that appear in the images because of the three–dimensional scour surface have been corrected with geometrical data of the sediment bed.

As first results the averaged movement directions and the histograms of the movements in certain areas have been presented for the scouring stages after 0.5 h and 12 h at a high spatial resolution. The figures show the different dominant scouring agents in a small, rapidly growing and in a developed scour hole. Also the regions with the highest numbers of transported grains are detected.

REFERENCES

Dargahi, B. (1987) Flow field and local scouring around a cylinder. Hydraulics Laboratory, The Royal Institute of Technology, Stockholm, Sweden

Dey, S. (1999) Time-variation of scour in the vicinity of circular piers. Proc Instn Civ Engrs Wat, Marit & Energy 136:67-75

Hjorth, P. (1975) Studies on the nature of local scour. PhD thesis, University of Lund

Keshavarzy, A., Ball, J. (1999) An application of image processing in the study of sediment motion. Journal of Hydraulic Research 37(4):559-576

Kirkil, G., Constantinescu, G., Ettema, R. (2008) Coherent structures in the flow field around a circular cylinder with scour hole. Journal of Hydraulic Engineering 134(5):572-587

Link, O. (2006) Untersuchung der Kolkung an einem schlanken zylindrischen Pfeiler in sandigem Boden. PhD thesis, Technische Universität Darmstadt, Darmstadt

Link, O., Gobert, C., Manhart, M., Zanke, U. (2008a) Effect of the horseshoe vortex system on the geometry of a developing scour hole at a cylinder. In: 4th International Conference on Scour and Erosion, Tokyo

Link, O., Pfleger, F., Zanke, U. (2008b) Characteristics of developing scour holes at a sand-embedded cylinder. International Journal of Sediment Research 23(3):258-266

Melville, B.W. (1975) Local scour at bridge sites. PhD thesis, University of Auckland

Papanicolaou, A.N., Diplas, P., Balakrishnan, M., Dancey, C.L. (1999) Computer vision technique for tracking bed load movement. Journal of Computation in Civil Engineering pp 71-79

Pilotti, M., Menduni, G., Castelli, E. (1997) Monitoring the inception of sediment transpot by image processing techniques. Experiments in Fluids 23:202-208

Radice, A., Ballio, F., Armenio, V., Franzetti, S. (2006a) Scour development and sediment motion at rectangular and trapezoidal abutments. In: Verheij, H., Hoffmans, G. (eds) Proceedings to ICSE 3, 3rd International Conference on Scour and Erosion, CURNET, Gouda, The Netherlands, pp 547-555

Radice, A., Malavasi, S., Ballio, F. (2006b) Solid transport measurements through image processing. Exp Fluids 41:721-734

Radice, A., Malavasi, S., Ballio, F. (2008) Sediment kinematics in abutment scour. Journal of Hydraulic Engineering 134(2):146-156

Sechet, P., LeGuennec, B. (1999) Bursting phenomenon and incipient motion of solid particles in bed-load transport. Journal of Hydraulic Research 37(5):683-696

van Rijn, L. C. (1984) Sediment Transport, Part I: Bed Load Transport. Journal of Hydraulic Engineering 110(10):1431-1456

Zanke, U. (1982) Kolke am Pfeiler in richtungskonstanter Strömung und unter Welleneinfluss. Mitteilungen des Franzius-Instituts für Wasserbau- und Küsteningenieurwesen der Universität Hannover 54:381-416